Ab Initio Calculation of Entropy and Heat Capacity of Gas-Phase *n*-Alkanes Using Internal Rotations

P. Vansteenkiste,*,† V. Van Speybroeck,‡ G. B. Marin,‡ and M. Waroquier†

Laboratory of Theoretical Physics, Ghent University, Proeftuinstraat 86, B-9000 Gent, Belgium, and Laboratorium van Petrochemische Techniek, Ghent University, Krijgslaan 281, B-9000 Gent, Belgium

Received: October 4, 2002; In Final Form: February 6, 2003

This work attempts to improve the theoretical reproduction of thermodynamic properties, such as entropies and heat capacities of gas-phase *n*-alkanes, by using a more precise quantum-mechanical treatment of the internal rotations. Present ab initio methods all handle the internal modes in the harmonic oscillator approach. It has already been noted that this approach underestimates the microscopic partition functions (Van Speybroeck et al., *J. Phys. Chem. A* **2000**, *104*, 10939). In this work, an uncoupled scheme for internal rotations is applied to a large number of *n*-alkanes within the DFT formalism at the B3LYP/6-311g** level. The method being examined in this paper drastically improves the agreement between theoretical and experimental thermodynamic properties. Moreover, the method has been shown to be efficient and to be easily implemented in each ab initio software package.

Introduction

Ab initio calculations provide a highly appropriate way to calculate various thermodynamic properties, such as the entropy and heat capacity, by statistical mechanics. Basic quantities are the microscopic partition functions related to all degrees of freedom present in the molecule, as the overall translation and rotation of the molecule and the remaining internal vibrational modes. In standard ab initio codes, all internal vibrational modes are treated within the harmonic oscillator approach. However, in previous work of the authors,[1−3] the importance of treating low vibrational modes in a more appropriate way was shown. As the molecule gets larger, the number of vibrational degrees of freedom increases and the contribution of internal rotations to the total entropy and other thermodynamic properties becomes larger. The larger the molecule, the higher the sensitivity of the approximations applied to calculate the partition function.

In this paper, we show that even the most straightforward method of describing internal rotational modes, which is based upon one-dimensional rotational potentials, obtained from ab initio calculations, drastically improves the accuracy of reproducing thermodynamic properties. The goal of this paper is to apply the uncoupled model, outlined in previous work of the authors,[1−3] on *n*-alkanes up to decane and to study its influence on the reproduction of the entropy and heat capacity, for which good experimental values are available. A more elaborate treatment of subsequent internal rotations in a coupled scheme is feasible[1,5] but requires a high numerical cost in the construction of multidimensional torsional potential surfaces. This general scheme is not of practical use to implement in present ab initio codes but gives an indication of the reliability of the various approximations that may be applied to the general scheme. Such generalization is outside the scope of the present study. This paper primarily aims at emphasizing the importance of considering more elaborate treatments of low vibrational modes. They mostly correspond with quasi-free or hindered rotations of part of the molecule about a single bond.

n-Alkanes constitute an ideal series of molecules to test the influence of internal rotations on thermodynamic properties. They contain methylene sequences with a chain of subsequent internal rotations. In addition, accurate experimental estimates for the entropy and heat capacity are available at various temperatures and in the range from ethane to decane.[6−9] East and Radom[10] carried out an extensive study of small molecules at different levels of ab initio molecular orbital theory and different methods for calculating entropies and showed that entropies could be calculated to within 1 (J/K)/mol. Therefore, they used high levels of theory (ranging from MP2/6-31G(d) to MP2/6-311+G(2df,p)) and treated individual internal rotations explicitly with a cosine potential based on barrier heights of the torsional potential. Their method differs from the presented one in the number of contributions in the Fourier fit in reproducing the torsional potential.

Another recent paper regarding the ab initio calculation of the entropy of gas-phase organic molecules is the work of Guthrie.[11] Entropy values are calculated at the B3LYP/6-31G** level of theory with an overall standard deviation of 5.35 (J/K)/mol in entropy at 298.15 K. The training set consisted of 128 molecules with particular focus on relatively large molecules with up to 10 carbon atoms. In the work of Guthrie, the calculated entropy values have been adjusted by an empirical correction term that accounts for various low-lying conformations. This study reports values of entropies that are quite satisfactory, emphasizing the adequacy of density functional theory (DFT)-like models in reproducing thermodynamic properties with an acceptable accuracy.

Methodology and Computational Details

All ab initio calculations were performed using the Gaussian98 software package.[12] All optimizations, frequency calculations, and potential scans were done using DFT,[13] with Becke's three-parameter B3LYP functional.[14] The molecular orbitals were expanded in a triple-ζ 6-311G basis augmented with single first d and p polarization functions.[15] This functional is known to give a reliable and quantitatively acceptable description of geometries, frequencies, and potentials[16−18] for a reasonable computation time. In particular, a profound

---

* To whom all correspondence should be addressed. Tel: +32 (0)9 264 65 63. E-mail: peter.vansteenkiste@rug.ac.be.

† Laboratory of Theoretical Physics.

‡ Laboratorium van Petrochemische Techniek.

10.1021/jp027132u CCC: $25.00

quantum chemical study of conformational energies and rotational energy barriers was performed by Smith and Jaffe in *n*-alkanes using high-level ab initio methods.[19] As will be discussed later, a comparative study between their results and ours shows that the agreement is remarkable even on the quantitative level. The frequency calculation gives all normal modes of the molecule and enables us to select those vibrational modes that correspond with internal rotations. In the uncoupled scheme adopted in this work, the one-dimensional rotational potential is calculated for the selected modes by performing a scan in terms of the relevant torsional angle and relaxing all other degrees of freedom. This procedure is slightly different with that applied by the authors in previous work,[2,3] where the potential is determined by some stationary points, corresponding with a full geometry optimization. The latter scheme is expected to yield more realistic values of the rotational barriers,[4,20] and the barrier heights resulting from the scan procedure are in good agreement with the high-level ab initio predictions, as will be shown later in the discussion. The final potential is then obtained by fitting a cosine series through the calculated data points:

$$V_i(\phi_i) = \sum_{j=1}^{18} a_{ij}(1 - \cos(j\phi_i)) \tag{1}$$

with index *i* standing for the identification of the particular internal rotation under consideration. The partition function can now be obtained quantum mechanically or classically dependent on the temperature range of interest. For low temperatures (below 400 K), a quantum mechanical treatment is needed and one has to solve the one-dimensional Schrödinger equation

$$\left[-\frac{\hbar^2}{2\beta_i}\frac{\partial^2}{\partial\phi_i^2} + V_i(\phi_i)\right]\psi_{ki}(\phi_i) = \epsilon_{ki}\psi_{ki}(\phi_i) \tag{2}$$

This is done by the numerical procedure as outlined in ref 3, yielding all rotational energy eigenvalues ϵ_{ki} required for the evaluation of the partition function of internal rotation *i* defined by

$$q_i = \frac{1}{\sigma_i}\sum_k g_k e^{-\epsilon_{ki}/(kT)} \tag{3}$$

with σ_i the symmetry number of the rotational top and g_k the degeneracy of the energy level *k*. The quantity β_i in the one-dimensional Schrödinger equation represents the generalized reduced moment of inertia of an asymmetric top as defined in ref 21. For symmetric tops it reduces to

$$\beta_i = I_i\left(1 - \sum_k \gamma_k^2 \frac{I_i}{I_{gl,k}}\right) \tag{4}$$

with γ_k the direction cosines between the rotational axis and the axes of inertia of the global molecule, I_i the moment of the top, and $I_{gl,k}$ the moments of inertia of the global molecule.[21] For temperatures above 500 K, the quantum mechanical and classical partition functions are expected to converge. The classical partition function is obtained as an integral:[22]

$$q_i = \frac{1}{\sigma_i}\frac{\sqrt{2\pi kT\beta_i}}{h}\int e^{-V_i(\phi_i)/(kT)}\, d\phi_i \tag{5}$$

Finally, the partition functions as determined in the harmonic oscillator approach are replaced by the new values. Knowledge of the total molecular partition function allows us to evaluate macroscopic thermodynamic quantities, such as the entropy

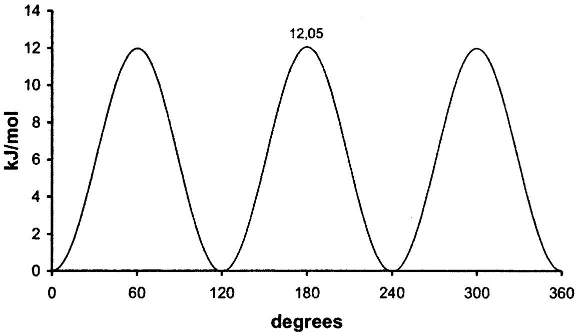

Figure 1. Potential of methyl rotation in pentane relative to the energetically most favored conformation (trans).

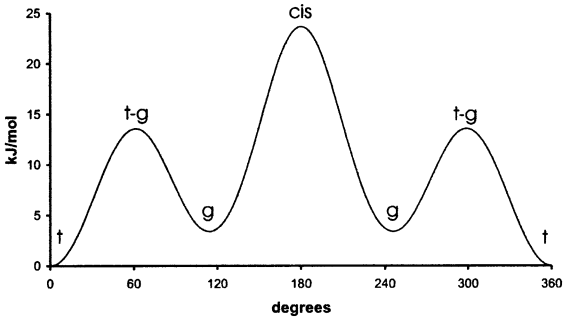

Figure 2. Potential of the ethyl rotation in butane relative to the energetically most favored conformation.

$$S = R\left(\ln q + T\left(\frac{\partial \ln q}{\partial T}\right)\right) \tag{6}$$

and the heat capacity

$$C = RT\left(2\frac{\partial \ln q}{\partial T} + T\frac{\partial^2 \ln q}{\partial T^2}\right) \tag{7}$$

Results and Discussion

1. Torsional Potentials. In *n*-alkanes, two classes of rotational potentials are present: one corresponding with rotations of ending methyl groups (Figure 1) and another associated with CCCC carbon torsional variations (Figure 2).

The potential of the methyl rotation has a 3-fold symmetry and is determined by only one parameter, the relative potential barrier height; the reference conformation is defined as the all-trans conformation. This parameter is plotted for the different alkanes in Figure 3. The relative potential barrier height seems to converge to a value of ~12 kJ/mol for the larger chains. This convergence can be expected since, as the chain length increases, the tops do not feel the effect of the other methyl end but only of the closest CH_2 groups. The inner rotational potentials all show a general behavior as schematically presented in Figure 2. The reference trans equilibrium (t) conformation at $\phi = 0°$ is separated from the higher energy gauche conformation (g) ($\phi \approx 115°$) by the t−g barriers (60°), while direct transition between the gauche states requires traversing the cis barrier ($\phi = 180°$). The energy difference between the trans and gauche conformations has been the subject of much debate in the past, from both experimental and theoretical points of view.[19] It is also an interesting issue to find out whether convergence is achieved for the gauche energy and barrier heights in larger *n*-alkanes. Although this is not the topic of

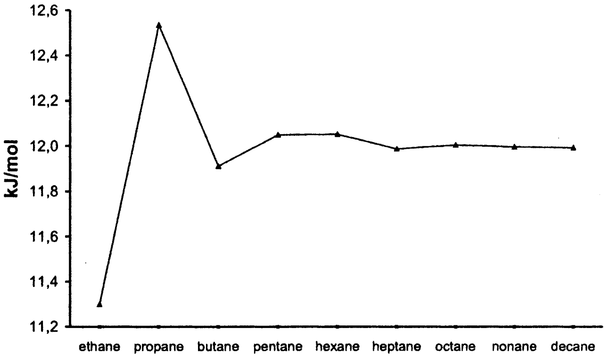

Figure 3. Potential barrier height of the ending methyl rotation relative to the energetically most favored conformation.

TABLE 1: Gauche Energy and t−g and Cis Rotational Energy Barriers in *n*-Butane and *n*-Hexane

	MP2/6-311G**[a] (kJ/mol)	MP2/6-311G(2 gf,p)//CCSD(T)[a] (kJ/mol)	Herrebout et al.[b] (kJ/mol)	B3LYP/ 6-311G**[c] (kJ/mol)
		n-Butane		
t	0.00	0.00		0.00
t−g	14.22	13.85		13.58
g	2.13	2.26	2.80	3.45
cis	24.77	22.93		23.67
		n-Hexane		
t	0.00			0.00
t−g	12.09			12.95
g	1.84		2.18	3.52
cis	23.55			23.69

[a] Reference 19. [b] Reference 23. [c] This work.

the present paper, some preliminary conclusions may still be drawn. Many ab initio calculations of the gauche energy in *n*-alkanes have been performed.[23,24−28] An overview of the different results is given in ref 19. We report in Table 1 the most advanced results of the gauche energy and the t−g and cis rotational energy barriers in *n*-butane and *n*-hexane. The B3LYP/6-311G** predictions of the barriers agree quite well with those obtained with very high-level computational calculations such as MP2/6-311G(2gf,p)//CCSD(T). The differences between the cis and the t−g barriers are very well reproduced, and this agreement strengthens the reliability of our predictions of the entropy corrections due to the internal rotations on the quantitative level. On the other hand, the gauche energies are somewhat overestimated, but it is expected that those energies have little influence on the rotational energy levels as obtained from the eigenvalue equation (eq 2).

To check this assumption, we used the gauche energy value from ref 23 to calculate the energy levels of the inner rotation of hexane. This slight change lowers the ground rotational energy level by 1.2%, while the decrease of the higher energy levels is even smaller (1%). These small changes give rise to an increase of the entropy by ∼0.2 (J/K)/mol at 300 K, while at higher temperatures, the results are unaffected. The values of the heat capacity are somewhat more influenced: a decrease of ∼0.9 (J/K)/mol at 300 K, while at 1500 K, there is an increase of 0.05 (J/K)/mol, bringing the calculated values closer to experiment. The variations, however, are still very small. These results ensure that the potential values obtained by the B3LYP functional have enough accuracy for the goal of this paper. The different parameters characterizing the gauche and cis conformation (g and cis) are plotted in Figures 4 and 5 for the various internal rotations of the C−C−C−C torsional angle in terms of the length of the alkyl chain.

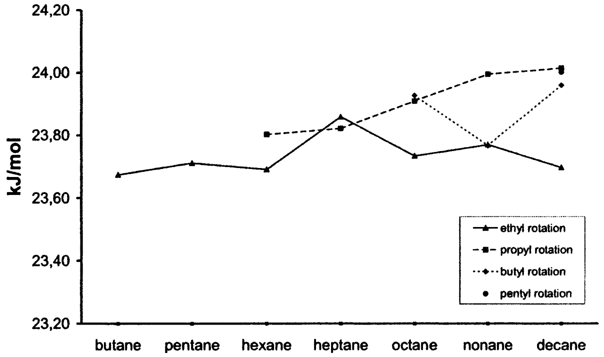

Figure 4. Cis barriers relative to the trans conformation.

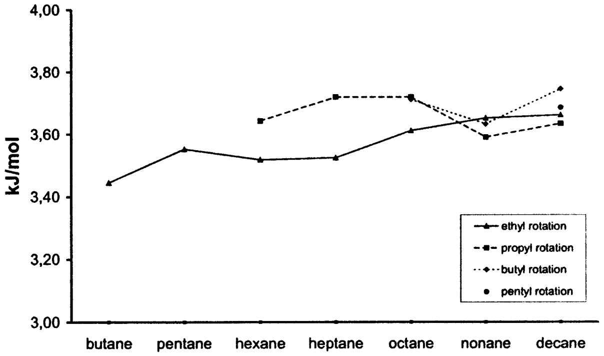

Figure 5. Local minimum heights at gauche conformation relative to the trans conformation.

The cis conformation is always located at a torsional angle of 180° due to the symmetry of the rotational potential. This means that the energies resulting from our scan equal those obtained from full geometry optimizations toward a transition state. Convergence of the cis barrier height is obtained within 0,05−0,07 kJ/mol, which is within the numerical accuracy. Not only convergence within each class of internal rotations is present, but also the values of the cis barriers of the propyl, butyl, and pentyl rotations are converged in decane. This was expected, since the larger the alkyl chain, the smaller the effect of the boundaries on the specific internal rotation.

The gauche conformation is not always located at the same position of the torsional angle for the different internal rotations and for the various alkanes. In our scan, a local minimum was found at 115°. To find the real gauche state, we performed optimizations starting from this 115° geometry. The resulting relative energy values of these stationary points are shown in Figure 5. Again convergence up to 0,05 kJ/mol is achieved in terms of the length of the alkyl chain. Moreover in decane, the relative gauche energies associated with the various torsional motions are also converged within the numerical accuracy.

In this work, we adopt the uncoupled scheme. In other words, all torsional potentials are one-dimensional, and for large deviations from the equilibrium values of the torsional angles in the chain, we can expect that the uncoupled representations of subsequent internal rotations may seriously differ from the multidimensional scheme. Conformers with several gauche configurations (such as gtg, gg, ggg, ...) are probably not very well described in this approximation. We refer to ref 29 for a thorough discussion about the stability of those conformers. Nevertheless, we want to emphasize that our calculations give evidence for slight changes in the geometry in the applied constrained optimization procedure. If the constraint concerns one torsional angle, the relaxation affects the original conformation to a very small extent, and in addition, the relaxation only

TABLE 2: Entropy and Heat Capacity of Ethane[a]

	temp (K)	H.O.	I.R.$^{\text{Q.M.}}$	I.R.$^{\text{Cl.}}$	exptl
S	298.15	227.770	229.011	228.349	229.161[b]
	300	228.083	229.331	228.677	229.487[b]
	400	244.385	245.912	245.547	246.378[b]
	500	259.940	261.526	261.304	262.344[b]
	600	274.913	276.411	276.267	277.568[b]
	700	289.288	290.610	290.513	292.080[b]
	800	303.053	304.154	304.085	305.904[b]
	900	316.218	317.073	317.022	319.075[b]
	1000	328.800	329.401	329.363	331.628[b]
	1100	340.824	341.170	341.141	343.597[b]
	1200	352.316	352.410	352.387	355.012[b]
	1300	363.301	363.151	363.133	365.908[b]
	1400	373.808	373.421	373.406	376.314[b]
	1500	383.864	383.249	383.237	386.260[b]
C_p	298.15	50.52	51.73	53.00	52.49[c]
	300	50.74	51.94	53.20	52.71[c]
	400	63.44	64.08	64.86	65.46[c]
	500	76.32	76.19	76.70	77.94[c]
	600	88.07	87.23	87.58	89.19[c]
	700	98.49	97.06	97.31	99.14[c]
	800	107.70	105.81	105.99	107.94[c]
	900	115.83	113.57	113.70	115.71[c]
	1000	122.99	120.44	120.54	122.55[c]
	1100	129.29	126.50	126.58	128.55[c]
	1200	134.81	131.83	131.89	133.80[c]
	1300	139.64	136.51	136.56	138.39[c]
	1400	143.88	140.62	140.66	142.40[c]
	1500	147.59	144.23	144.27	145.90[c]

[a] Entropy in units of (J/K)/mol; heat capacity in units of (J/K)/mol. [b] Experimental entropy values obtained from ref 7. [c] Experimental heat capacity values obtained from ref 6.

TABLE 3: Entropy and Heat Capacity of Propane[a]

	temp (K)	H.O.	I.R.$^{\text{Q.M.}}$	I.R.$^{\text{Cl.}}$	exptl
S	298.15	268.645	271.013	270.120	270.313[a]
	300	269.081	271.466	270.583	270.769[a]
	400	292.079	295.164	294.666	294.739[a]
	500	314.335	317.728	317.421	317.768[a]
	600	335.862	339.252	339.051	339.753[a]
	700	356.546	359.727	359.590	360.668[a]
	800	376.338	379.186	379.088	380.528[a]
	900	395.237	397.682	397.610	399.381[a]
	1000	413.271	415.276	415.222	417.293[a]
	1100	430.476	432.025	431.983	434.321[a]
	1200	446.892	447.983	447.950	450.526[a]
	1300	462.564	463.201	463.175	465.961[a]
	1400	477.535	477.727	477.706	480.675[a]
	1500	491.847	491.606	491.589	494.721[a]
C_p	298.15	70.33	73.00	74.70	73.60[b]
	300	70.68	73.34	75.03	73.93[b]
	400	90..35	92.34	93.38	94.01[b]
	500	109.57	110.24	110.93	112.59[b]
	600	126.72	125.98	126.47	128.70[b]
	700	141.69	139.71	140.06	142.67[b]
	800	154.74	151.74	151.99	154.77[b]
	900	166.15	162.32	162.51	165.35[b]
	1000	176..12	171.62	171.77	174.60[b]
	1100	184.84	179.79	179.91	182.67[b]
	1200	192.45	186.96	187.05	189.74[b]
	1300	199.09	193.24	193.31	195.85[b]
	1400	204.89	198.74	198.80	201.21[b]
	1500	209.96	203.56	203.61	205.89[b]

[a] Entropy in units of (J/K)/mol; heat capacity in units of (J/K)/mol. [b] Experimental entropy values obtained from ref 7. [c] Experimental heat capacity values obtained from ref 6.

TABLE 4: Entropy and Heat Capacity of Butane[a]

	temp (K)	H.O.	I.R.$^{\text{Q.M.}}$	I.R.$^{\text{Cl.}}$	exptl
S	298.15	300.760	311.082	310.138	309.910[b]
	300	301.323	311.689	310.756	310.746[c]
	400	331.110	343.208	342.686	
	500	360.083	372.934	372.614	372.794[c]
	600	388.156	401.150	400.941	
	700	415.137	427.910	427.767	428.986[c]
	800	440.942	453.281	453.180	
	900	465.566	477.352	477.278	
	1000	489.042	500.212	500.155	502.749[c]
	1100	511.420	521.942	521.899	
	1200	532.757	542.622	542.587	
	1300	553.111	562.321	562.294	
	1400	572.542	581.108	581.086	
	1500	591.107	599.045	599.026	
C_p	298.15	90.69	97.87	99.69	98.49[d]
	300	91.15	98.29	100.09	98.95[d]
	400	117.41	122.09	123.19	124.77[d]
	500	142.81	144.80	145.53	148.66[d]
	600	165.30	164.87	165.38	169.28[d]
	700	184.79	182.36	182.72	187.02[d]
	800	201.69	197.65	197.91	202.38[d]
	900	216.39	211.06	211.25	215.73[d]
	1000	229.18	222.82	222.97	227.36[d]
	1100	240.32	233.12	233.24	237.48[d]
	1200	250.02	242.14	242.23	246.27[d]
	1300	258.48	250.02	250.10	253.93[d]
	1400	265.84	256.92	256.99	260..58[d]
	1500	272.28	262.97	263.02	266.40[d]

[a] Entropy in units of (J/K)/mol; heat capacity in units of (J/K)/mol. [b] Experimental entropy value obtained from ref 8. [c] Experimental entropy values obtained from ref 9. [d] Experimental heat capacity values obtained from ref 6.

has effect on the closest neighbors. Anyway, an explicit application of the coupled scheme is recommended in order to draw general conclusions about the adequacy of the uncoupled scheme to predict entropy corrections due to internal rotations on a high quantitative level. Those calculations are very time-consuming and are in progress.[5]

2. Entropy and Heat Capacity. We report the calculated values of the entropy and heat capacity for the *n*-alkanes in Tables 2−10, together with the experimental values over a large temperature range. We distinguish between the predictions made in a quantum mechanical approach (by solving eq 2) and those obtained by evaluating the classical integral of eq 5. These results are respectively indicated by I.R.$^{\text{Q.M.}}$ and I.R.$^{\text{Cl.}}$. For low temperatures, the quantum mechanical approach is recommended, but for high temperatures, both values are converging. When treating internal rotations, we notice a systematic increase of the two thermodynamic quantities at low temperature with regard to the theoretical predictions within the harmonic oscillator (H.O.) model, while at higher temperatures the heat capacity is lower than the one predicted by the H.O. model. In Figure 6, the entropy at room temperature and at 1000 K is plotted throughout the whole range of the *n*-alkanes under study. The overall agreement with experiment is remarkable. The H.O. predictions for the entropy systematically underestimate the experimental values. The discrepancies increase with the length of the alkyl chain. The corrections predicted by the I.R. model bring the theoretical predictions very close to the experimental values. The corrections are larger for the longer *n*-alkanes, in this way compensating the larger discrepancies noticed in the H.O. results. The observation that the corrections due to the inclusion of internal rotations are systematically increasing with the length of the chain is not surprising, but the fact that the magnitude of these correction terms almost coincides with the deviation of the H.O. results from the experiment is spectacular and gives a clear indication of the inadequacy of the H.O. model to predict reliable microscopic properties in molecules that contain a large number of internal rotations. The H.O. approximation also fails in reproducing a correct temperature dependence of the heat capacity. At low temperatures, the H.O.

TABLE 5: Entropy and Heat Capacity of Pentane[a]

	temp (K)	H.O.	I.R.$^{Q.M.}$	I.R.$^{Cl.}$	exptl
S	298.15	332.899	350.830	349.840	349.450[b]
	300	333.587	351.592	350.613	349.699[c]
	400	370.142	390.978	390.429	
	500	405.810	427.881	427.544	426.266[c]
	600	440.411	462.800	462.579	
	700	473.676	495.851	495.701	495.469[c]
	800	505.485	527.144	527.036	
	900	535.826	556.797	556.718	
	1000	564.738	584.928	584.868	586.137[c]
	1100	592.285	611.647	611.600	
	1200	618.538	637.054	637.017	
	1300	643.571	661.240	661.210	
	1400	667.460	684.293	684.268	
	1500	690.277	706.290	706.270	
C_p	298.15	110.99	122.96	124.87	120.00[d]
	300	111.57	123.46	125.35	120.62[d]
	400	144.37	151.93	153.08	152.55[d]
	500	175.96	179.42	180.18	182.59[d]
	600	203.79	203.81	204.34	208.78[d]
	700	227.82	225.07	225.45	231.38[d]
	800	248.57	243.62	243.90	250.62[d]
	900	266.56	259.86	260.07	266.94[c]
	1000	282.19	274.08	274.24	281.58[d]
	1100	295.76	286.51	286.64	293.72[d]
	1200	307.57	297.38	297.48	304.60[d]
	1300	317.83	306.88	306.96	313.80[d]
	1400	326.77	315.17	315.24	322.17[d]
	1500	334.58	322.43	322.49	330.54[d]

[a] Entropy in units of (J/K)/mol; heat capacity in units of (J/K)/mol. [b] Experimental entropy value obtained from ref 8. [c] Experimental entropy values obtained from ref 9. [d] Experimental heat capacity values obtained from ref 6.

TABLE 6: Entropy and Heat Capacity of Hexane[a]

	temp (K)	H.O.	I.R.$^{Q.M.}$	I.R.$^{Cl.}$	exptl
S	298.15	365.034	390.995	389.986	388.820[b]
	300	365.849	391.915	390.918	389.321[c]
	400	409.206	439.244	438.685	
	500	451.601	483.376	483.033	480.407[c]
	600	492.756	525.030	524.806	
	700	532.322	564.396	564.242	562.664[c]
	800	570.146	601.624	601.514	
	900	606.212	636.868	636.786	
	1000	640.567	670.276	670.214	670.235[c]
	1100	673.287	701.986	701.938	
	1200	704.458	732.121	732.083	
	1300	734.172	760.795	760.764	
	1400	762.519	788.113	788.088	
	1500	789.587	814.172	814.150	
C_p	298.15	131.40	148.34	150.29	142.60[d]
	300	132.10	148.92	150.85	143.26[d]
	400	171.48	182.02	183.19	181.54[d]
	500	209.25	214.25	215.02	217.28[d]
	600	242.41	242.92	243.45	248.11[d]
	700	270.94	267.90	268.28	274.05[d]
	800	295.53	289.68	289.96	296.23[d]
	900	316.80	308.72	308.93	315.06[d]
	1000	335.23	325.38	325.54	331.37[d]
	1100	351.23	339.93	340.06	345.18[d]
	1200	365.13	352.64	352.74	357.31[d]
	1300	377.20	363.73	363.81	368.19[d]
	1400	387.71	373.42	373.48	376.56[d]
	1500	396.87	381.89	381.95	389.11[d]

[a] Entropy in units of (J/K)/mol; heat capacity in units of (J/K)/mol. [b] Experimental entropy value obtained from ref 6. [c] Experimental entropy values obtained from ref 9. [d] Experimental heat capacity values obtained from ref 6.

TABLE 7: Entropy and Heat Capacity of Heptane[a]

	temp (K)	H.O.	I.R.$^{Q.M.}$	I.R.$^{Cl.}$	exptl
S	298.15	397.030	430.597	429.578	427.980[b]
	300	397.971	431.673	430.667	428.944[c]
	400	448.107	486.936	486.372	
	500	497.206	538.287	537.941	534.590[c]
	600	544.896	586.669	586.442	
	700	590.750	632.341	632.186	629.901[c]
	800	634.581	675.498	675.387	
	900	676.366	716.329	716.246	
	1000	716.159	755.013	754.950	754.333[c]
	1100	754.048	791.712	791.662	
	1200	790.136	826.574	826.535	
	1300	824.528	859.735	859.703	
	1400	857.333	891.319	891.292	
	1500	888.653	921.438	921.415	
C_p	298.15	151.74	173.68	175.65	165.20[d]
	300	152.56	174.34	176.29	165.98[d]
	400	198.49	212.07	213.26	210.66[d]
	500	242.43	249.03	249.81	252.09[d]
	600	280.93	281.97	282.51	287.44[d]
	700	313.99	310.68	311.07	317.15[d]
	800	342.43	335.70	335.98	342.25[d]
	900	366.98	357.56	357.77	363.59[d]
	1000	388.25	376.66	376.82	381.58[d]
	1100	406.68	393.33	393.46	397.06[d]
	1200	422.67	407.88	407.98	410.45[d]
	1300	436.56	420.58	420.66	422.58[d]
	1400	448.64	431.66	431.73	435.14[d]
	1500	459.17	441.35	441.40	443.50[d]

[a] Entropy in units of (J/K)/mol; heat capacity in units of (J/K)/mol. [b] Experimental entropy value obtained from ref 8. [c] Experimental entropy values obtained from ref 9. [d] Experimental heat capacity values obtained from ref 6.

TABLE 8: Entropy and Heat Capacity of Octane[a]

	temp (K)	H.O.	I.R.$^{Q.M.}$	I.R.$^{Cl.}$	exptl
S	298.15	429.071	470.444	469.427	467.060[b]
	300	430.139	471.675	470.670	
	400	487.060	534.771	534.209	
	500	542.871	593.284	592.938	
	600	597.104	648.358	648.132	
	700	649.252	700.317	700.162	
	800	699.094	749.391	749.279	
	900	746.602	795.801	795.718	
	1000	791.835	839.755	839.691	
	1100	834.896	881.440	881.390	
	1200	875.902	921.028	920.988	
	1300	914.975	958.675	958.641	
	1400	952.239	994.522	994.494	
	1500	987.811	1028.702	1028.677	
C_p	298.15	172.10	198.66	200.62	187.80[c]
	300	173.03	199.40	201.34	188.70[c]
	400	225.52	241.82	243.00	239.74[c]
	500	275.65	283.58	284.37	286.81[c]
	600	319.50	320.87	321.40	326.77[c]
	700	357.08	353.35	353.74	360.24[c]
	800	389.36	381.65	381.93	388.28[c]
	900	417.20	406.34	406.55	411.71[c]
	1000	441.28	427.90	428.06	431.37[c]
	1100	462.14	446.71	446.83	448.52[c]
	1200	480.23	463.11	463.21	463.17[c]
	1300	495.93	477.42	477.49	476.98[c]
	1400	509.58	489.90	489.96	489.53[c]
	1500	521.47	500.80	500.85	497.90[c]

[a] Entropy in units of (J/K)/mol; heat capacity in units of (J/K)/mol. [b] Experimental entropy value obtained from ref 8. [c] Experimental heat capacity values obtained from ref 6.

predictions underestimate the experimental values, while at high temperatures, we notice an overestimation of the heat capacity, which is systematically increasing with the chain length. The behavior of the heat capacity as a function of the length of the chain also strongly depends on the temperature (Figure 7). Large discrepancies are noticed at low temperature. The corrections due to I.R. overshoot the experimental values. This is probably

TABLE 9: Entropy and Heat Capacity of Nonane[a]

	temp (K)	H.O.	I.R.$^{Q.M.}$	I.R.$^{Cl.}$	exptl
S	298.15	460.872	510.426	509.409	506.500[b]
	300	462.065	511.815	510.810	
	400	525.767	582.871	582.308	
	500	588.282	648.621	648.274	
	600	649.052	710.435	710.208	
	700	707.488	768.712	768.556	
	800	763.337	823.725	823.612	
	900	816.563	875.729	875.645	
	1000	867.234	924.964	924.899	
	1100	915.465	971.645	971.593	
	1200	961.387	1015.966	1015.923	
	1300	1005.140	1058.104	1058.068	
	1400	1046.861	1098.220	1098.190	
	1500	1086.685	1136.464	1136.437	
C_p	298.15	192.44	224.10	226.07	210.40[b]
	300	193.50	224.92	226.86	211.42[b]
	400	252.53	271.95	273.14	268.82[b]
	500	308.84	318.44	319.22	321.54[b]
	600	358.02	359.99	360.53	366.10[b]
	700	400.13	396.21	396.59	403.34[b]
	800	436.26	427.74	428.02	433.88[b]
	900	467.39	455.24	455.45	459.82[b]
	1000	494.30	479.24	479.40	481.58[b]
	1100	517.59	500.17	500.29	499.99[b]
	1200	537.77	518.41	518.51	516.31[b]
	1300	555.29	534.32	534.39	531.37[b]
	1400	570.51	548.19	548.25	543.92[b]
	1500	583.77	560.31	560.36	556.47[b]

[a] Entropy in units of (J/K)/mol; heat capacity in units of (J/K)/mol. [b] Experimental values obtained from ref 6.

TABLE 10: Entropy and Heat Capacity of Decane[a]

	temp (K)	H.O.	I.R.$^{Q.M.}$	I.R.$^{Cl.}$	exptl
S	298.15	492.902	550.087	549.077	545.800[b]
	300	494.222	551.633	550.634	546.096[c]
	400	564.710	630.615	630.055	
	500	633.938	703.574	703.229	695.381[c]
	600	701.250	772.107	771.881	
	700	765.980	836.686	836.529	829.771[c]
	800	827.841	897.623	897.509	
	900	886.790	955.210	955.124	
	1000	942.902	1009.717	1009.650	1004.871[c]
	1100	996.304	1061.384	1061.330	
	1200	1047.145	1110.430	1110.385	
	1300	1095.578	1157.052	1157.014	
	1400	1141.758	1201.432	1201.398	
	1500	1185.834	1243.735	1243.705	
C_p	298.15	212.80	249.44	251.40	233.10[d]
	300	213.97	250.34	252.27	234.18[d]
	400	279.58	301.97	303.14	297.98[d]
	500	342.07	353.17	353.95	356.43[d]
	600	396.59	399.00	399.53	405.85[d]
	700	443.22	438.95	439.33	446.43[d]
	800	483.19	473.72	474.00	479.90[d]
	900	517.61	504.04	504.25	508.36[d]
	1000	547.34	530.49	530.64	531.79[d]
	1100	573.06	553.54	553.66	551.87[d]
	1200	595.33	573.63	573.73	569.44[d]
	1300	614.66	591.14	591.21	585.76[d]
	1400	631.45	606.41	606.47	598.31[d]
	1500	646.07	619.74	619.79	610.86[d]

[a] Entropy in units of (J/K)/mol; heat capacity in units of (J/K)/mol. [b] Experimental entropy value obtained from ref 6. [c] Experimental entropy values obtained from ref 9. [d] Experimental heat capacity values obtained from ref 6.

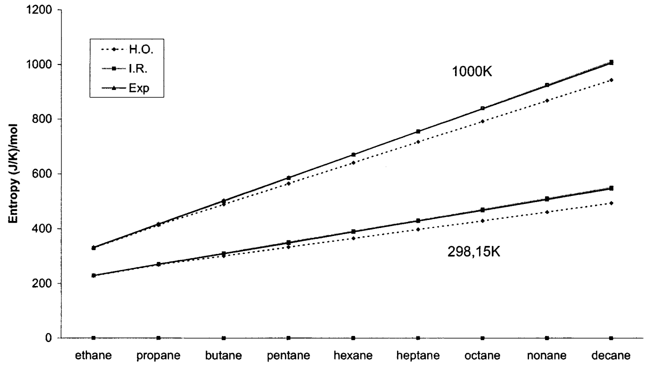

Figure 6. Entropy at 298.15 K and at 1000 K as a function of the chain length.

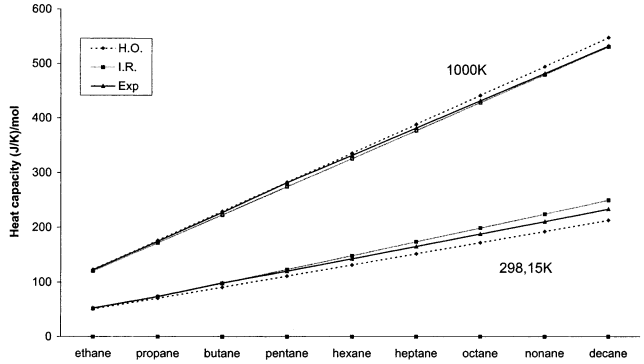

Figure 7. Heat capacity at 298.15 K and at 1000 K as a function of the chain length.

TABLE 11: Standard Deviations (%) of the Entropy (S)

	H.O.	I.R.$^{Q.M.}$	I.R.$^{Cl.}$
ethane	0.80	0.57	0.60
propane	0.90	0.42	0.42
butane	3.08	0.33	0.27
pentane	4.46	0.36	0.21
hexane	5.63	0.50	0.36
heptane	6.60	0.53	0.41
octane	8.17	0.69	0.47
nonane	9.01	0.78	0.57
decane	8.48	0.89	0.80

due to the use of the uncoupled scheme. In ref 1, it is already observed that a more rigorous coupled scheme may reduce the overall effect of treating internal rotations. A numerical verification of this assumption is in progress. To get an overall impression about the quantitative level of agreement regarding the reproduction of the entropy at various temperatures for the *n*-alkanes, we report in Table 11 the relative standard deviation defined by

$$\sigma = \left[\frac{1}{N}\sum\left(\frac{S^{\text{th}} - S^{\text{exp}}}{S^{\text{exp}}}\right)^2\right]^{1/2} \tag{8}$$

with N the number of data points. In the H.O. model, the standard deviation amounts to almost 10% for the higher alkanes, while in the I.R. approach, it remains constant and is less than 1%.

Conclusion

In this work, a model is presented to treat internal rotations in a very appropriate way. Although described in an uncoupled scheme, it has proved to be very efficient in evaluating corrections to the H.O. predictions on entropy and heat capacity in *n*-alkanes. The reproduction of the entropies is even that satisfactory that one would hardly expect better agreement when enhancing the level of the model. Subsequent internal rotations about a very long chain of single bonds require a more profound investigation of the coupling effects. This work is in progress.

Acknowledgment. This work is supported by the Fund for Scientific Research—Flanders (FWO) and the Research Board of Ghent University.

References and Notes

(1) Van Speybroeck, V.; Van Neck, D.; Waroquier, M. *J. Phys. Chem. A* **2002**, *106*, 8945.

(2) Van Speybroeck, V.; Borremans, Y.; Van Neck, D.; Waroquier, M.; Wauters, S.; Saeys, M.; Marin, G. B. *J. Phys. Chem. A* **2001**, *105*, 7713.

(3) Van Speybroeck, V.; Van Neck, D.; Waroquier, M.; Wauters, S.; Saeys, M.; Marin, G. B. *J. Phys. Chem. A* **2000**, *104*, 10939.

(4) Heuts, J. P. A.; Gilbert, R. G.; Radom, L. *J. Phys. Chem.* **1996**, *100*, 18997.

(5) Vansteenkiste, P.; Van Speybroeck, V.; Waroquier, M., in preparation.

(6) *N.I.S.T. Chemistry Webbook*,; http://webbook.nist.gov/.

(7) Lide, D. R., Frederikse, H. P. R., Eds. *CRC Handbook of Chemistry and Physics*, 74th ed.; CRC Press Inc.: Boca Raton, FL, 1995.

(8) *Entropy and Entropy of Formation of Gas*; http://www.knovel.com/.

(9) Stull, D. R.; Westrum, E. F.; Sinke, G. C. *The Chemical Thermodynamics of Organic Compounds*; John Wiley & Sons: New York, 1969.

(10) East, A. L. L.; Radom, L. *J. Chem. Phys.* **1997**, *106*, 6655.

(11) Guthrie, J. P. *J. Phys. Chem. A* **2001**, *105*, 8495.

(12) Frisch, M. J.; Trucks, G. W.; Schlegel, H. B.; Scuseria, G. E.; Robb, M. A.; Cheeseman, J. R.; Zakrzewski, V. G.; Montgomery, J. A., Jr.; Stratmann, R. E.; Burant, J. C.; Dapprich, S.; Millam, J. M.; Daniels, A. D.; Kudin, K. N.; Strain, M. C.; Farkas, O.; Tomasi, J.; Barone, V.; Cossi, M.; Cammi, R.; Mennucci, B.; Pomelli, C.; Adamo, C.; Clifford, S.; Ochterski, J.; Petersson, G. A.; Ayala, P. Y.; Cui, Q.; Morokuma, K.; Malick, D. K.; Rabuck, A. D.; Raghavachari, K.; Foresman, J. B.; Cioslowski, J.; Ortiz, J. V.; Stefanov, B. B.; Liu, G.; Liashenko, A.; Piskorz, P.; Komaromi, I.; Gomperts, R.; Martin, R. L.; Fox, D. J.; Keith, T.; Al-Laham, M. A.; Peng, C. Y.; Nanayakkara, A.; Gonzalez, C.; Challacombe, M.; Gill, P. M. W.; Johnson, B. G.; Chen, W.; Wong, M. W.; Andres, J. L.; Head-Gordon, M.; Replogle, E. S.; Pople, J. A. *Gaussian 98*; Gaussian, Inc.: Pittsburgh, PA, 1998.

(13) An example of a reference work: Parr, R. G.; Yang, W. *Density Functional Theory of Atoms and Molecules*; Oxford University Press: New York, 1989.

(14) Becke, A. D. *J. Chem. Phys.* **1993**, *98*, 5648.

(15) Krishnan, R.; Binkley, J. S.; Seeger, R.; Pople, J. A. *J. Chem. Phys.* **1980**, *72*, 650.

(16) Wong, M. W.; Radom, L. *J. Phys. Chem. A* **1998**, *102*, 2237.

(17) Parker, C. L.; Cooksy, A. L. *J. Phys. Chem. A* **1998**, *102*, 6186.

(18) Lynch, B. J.; Fast, P. L.; Harris, M.; Truhlar, D. G. *J. Phys. Chem. A* **2000**, *104*, 4811.

(19) Smith, G. D.; Jaffe, R. L. *J. Phys. Chem.* **1996**, *100*, 18718.

(20) Heuts, J. P. A.; Gilbert, R. G.; Radom, L. *Macromolecules* **1995**, *28*, 8771.

(21) Speybroeck, V. Van Ph.D. Thesis. Ab initio static and dynamic molecular methods: a useful tool in the study of chemical reactions. Ghent University, Ghent, 2001.

(22) McQuarrie, D. A. *Statistical Thermodynamics*; University Science Books: Mill Valley, CA, 1973.

(23) Herrebout, W. A.; van der Veken, B. J.; Wang, A.; Durig, J. R. *J. Phys. Chem.* **1995**, *99*, 578.

(24) Raghavachari, K. *J. Chem. Phys.* **1984**, *81*, 1383.

(25) Wiberg, K. B.; Murcko, M. A. *J. Am. Chem. Soc.* **1988**, *110*, 8029.

(26) Tsuzuki, S.; Schaefer, L.; Hitoshi, G.; Jemmis, E. D.; Hosoya, H.; Siam, K.; Tanabe, K.; Osawa, E. *J. Am. Chem. Soc.* **1991**, *113*, 4667.

(27) Mirkin, N. G.; Krimm, S. *J. Phys. Chem.* **1993**, *97*, 13887.

(28) Frey, R. F.; Cao, M.; Newton, S. Q.; Schaefer, L. *J. Mol. Struct. (THEOCHEM)* **1993**, *285*, 99.

(29) Koglin, E.; Meier, R. J. *J. Chem. Phys. Lett.* **1999**, *312*, 284.